

# Recent developments in understanding and modeling of defects in Czochralski germanium

J. Vanhellemont<sup>1</sup>, P. Spiewak<sup>2</sup>, E. Gaubas<sup>3</sup>, J. Lauwaert<sup>1</sup>, H. Vrielinck<sup>1</sup>, P. Clauws<sup>1</sup>, E. Simoen<sup>4</sup> and I. Romandic<sup>5</sup>

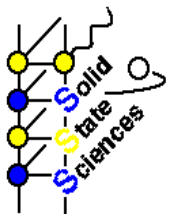
<sup>1</sup>Ghent University, Krijgslaan 281 S1, B-9000 Ghent, Belgium

<sup>2</sup>Warsaw University of Technology, Wołoska 141, 02-507 Warsaw, Poland

<sup>3</sup>Vilnius University, Sauletekio al 10, LT-10223 Vilnius, Lithuania

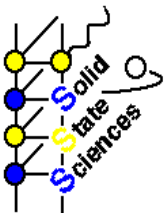
<sup>4</sup>Imec, Kapeldreef 75, B-3001 Leuven, Belgium

<sup>5</sup>Umicore EOM, Watertorenstraat 33, B-2250 Olen, Belgium



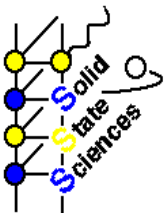
# Content

- Introduction
- COP's on polished Ge wafer surfaces
- Intrinsic point defects properties: experimental
- Calculation of intrinsic point defect properties
- Simulation of void formation in Cz germanium
- Conclusions

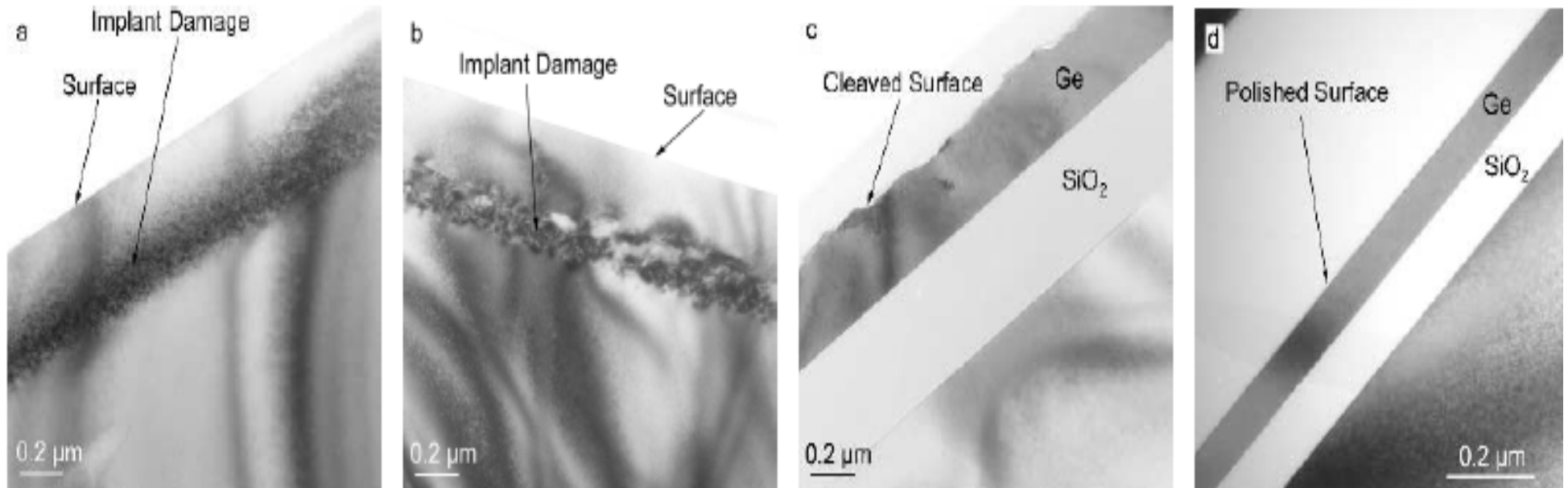


# Introduction

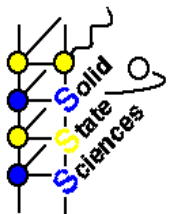
- Today main application of Ge substrates for GaAs epitaxy: highly doped, 100 mm diameter. Also for optical components (mirrors, lenses) and HR Ge for detectors.
- Renewed interest to use Ge in nano-electronics due to high carrier mobility.
- Limited reserves, high cost → GeOI.
- Development of electronics grade Cz Ge “donor” wafers:
  - grown-in lattice defects
  - metallic impurities
  - geometry.



# Bonded GeOI wafer



- XTEM of implanted Ge (a); after thermal treatment (b); after bonding and cleaving (c) and after CMP (d).



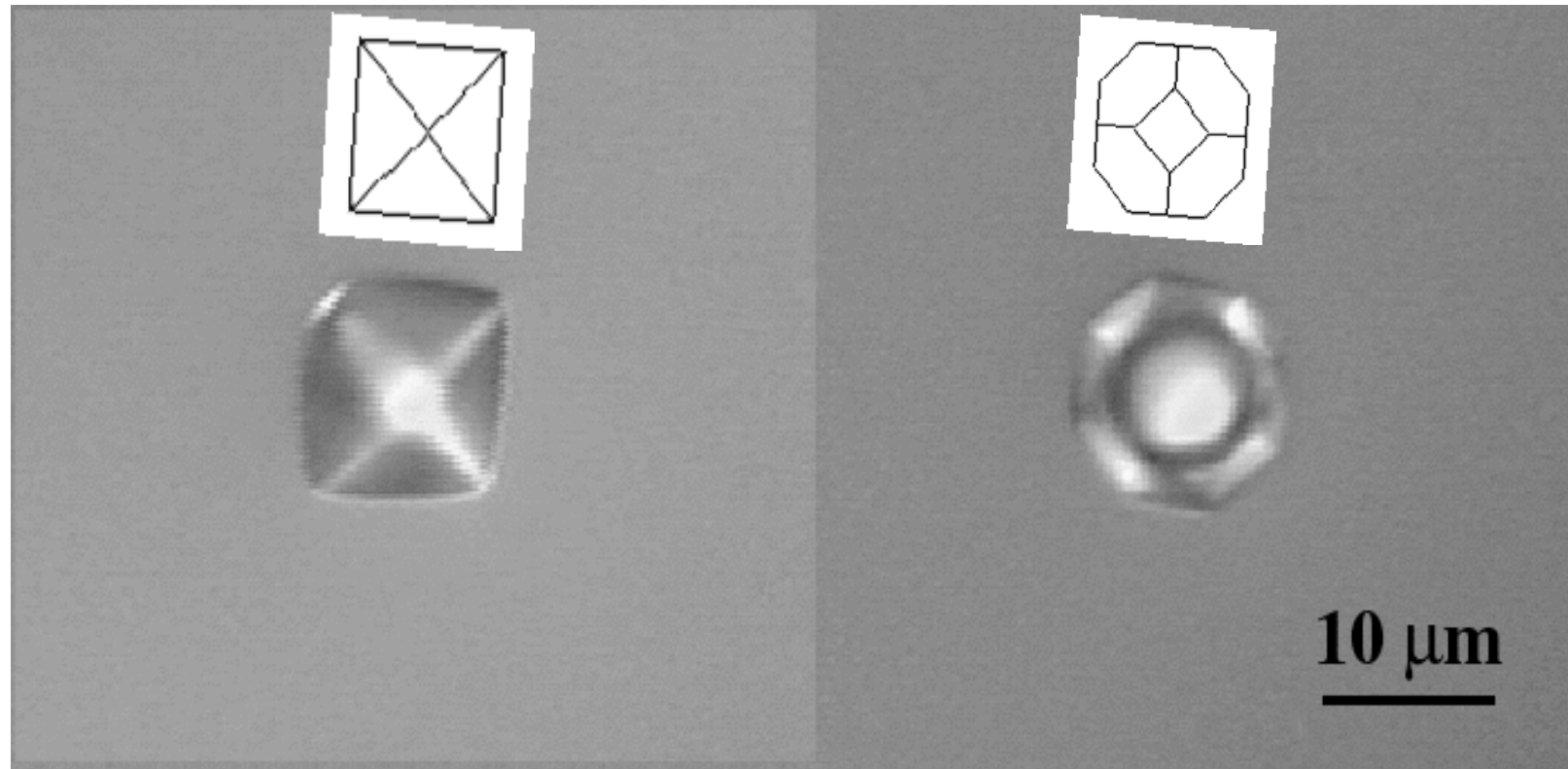
C.J. Tracy et al. Journ. Electron. Mater. **33**, 887 (2004)

# Cz germanium for nano-electronics



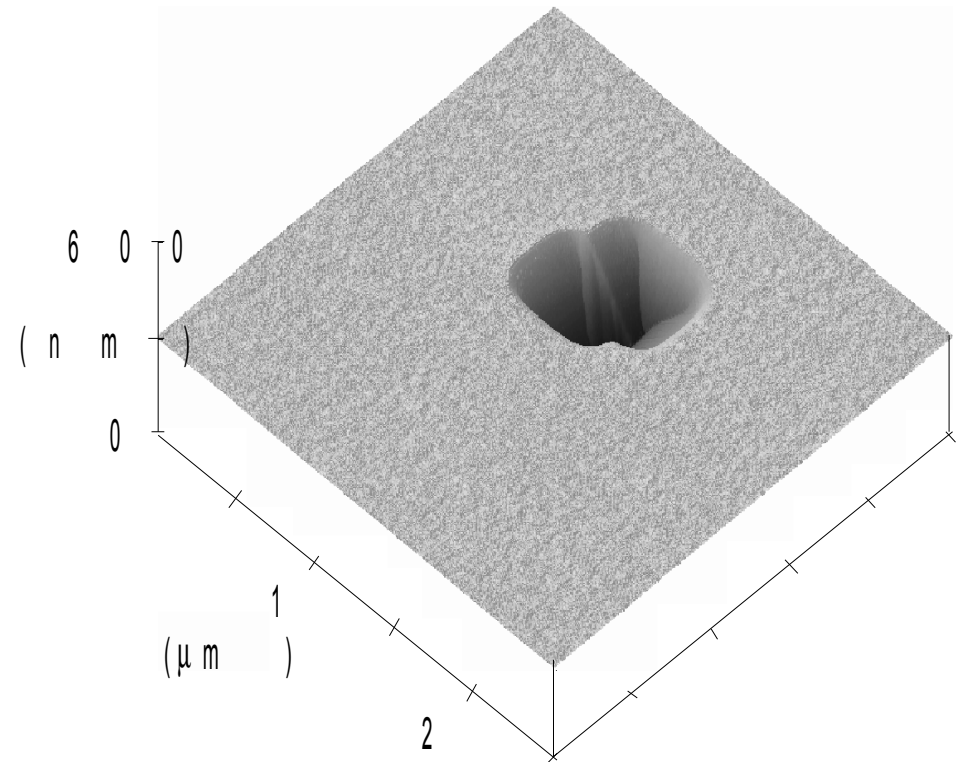
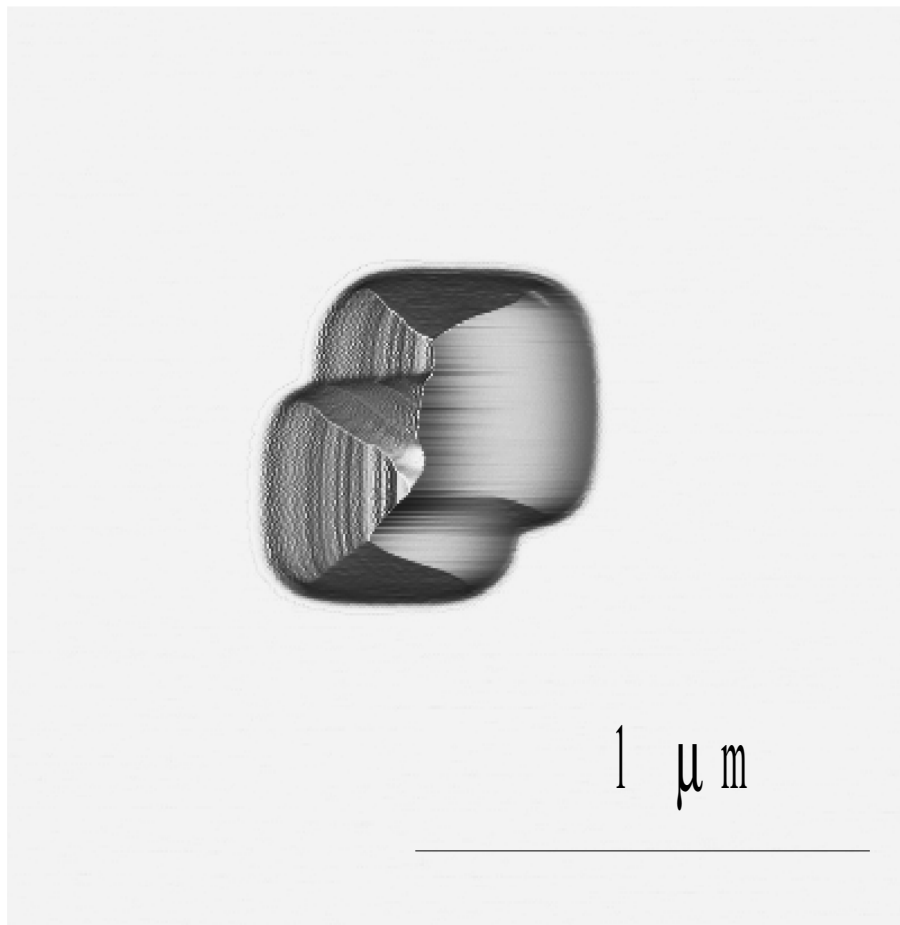
- 200 mm Ge wafers commercially available.
- Ge wafers fulfilling 300 mm wafer geometry specs demonstrated.
- Dislocation free; metals below detection limit.

# Surface pits on Cz germanium wafers



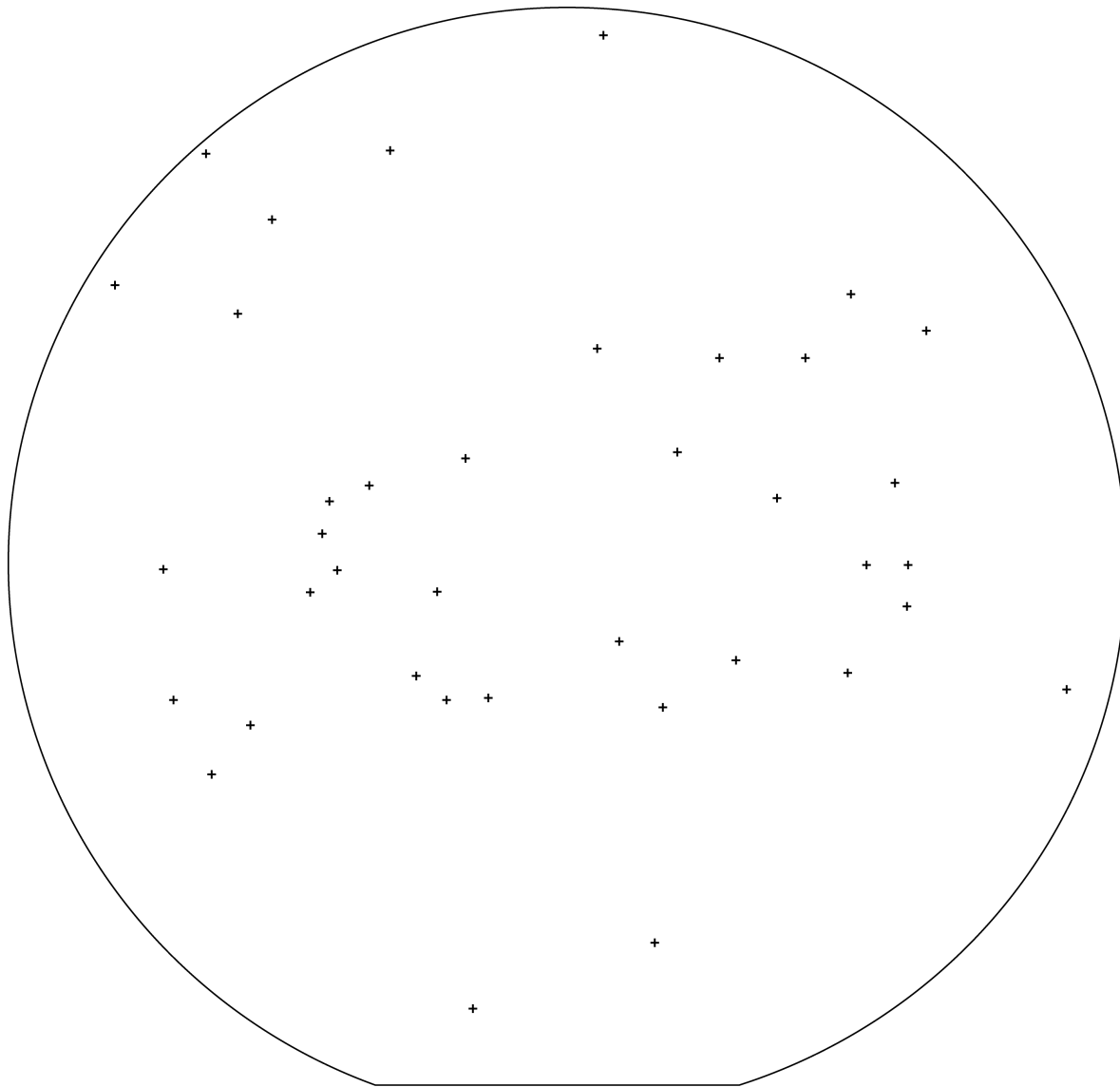
- Optical micrographs showing surface pits occasionally observed with the naked eye on Cz Ge wafer surfaces.

# COP'S on Cz silicon wafers



- AFM images of a typical double COP after 4h SC1 delineation. Left: top view. Right: 3D-view.

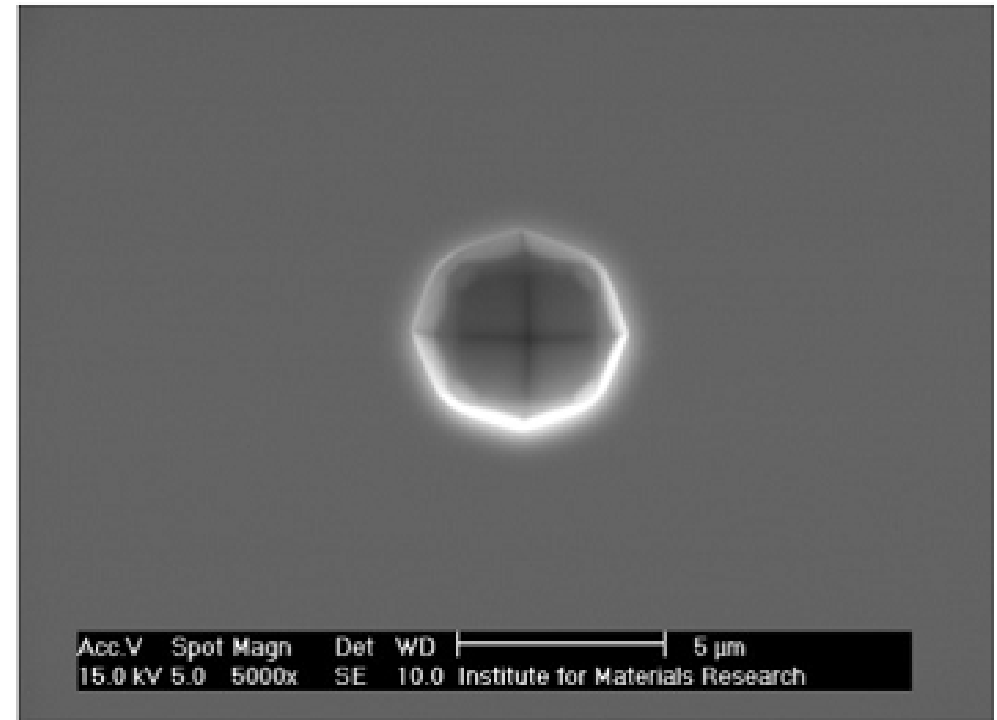
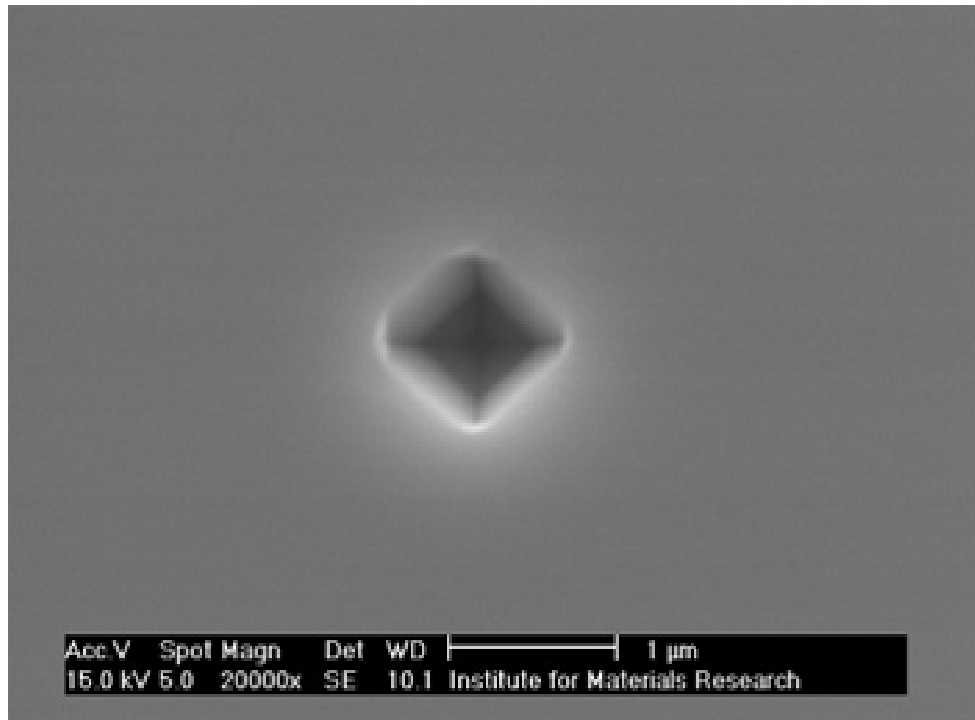
# COP'S on Cz germanium wafers?



- Image obtained with a SURFSCAN surface inspection tool, revealing the presence of large COP's on a polished germanium wafer.

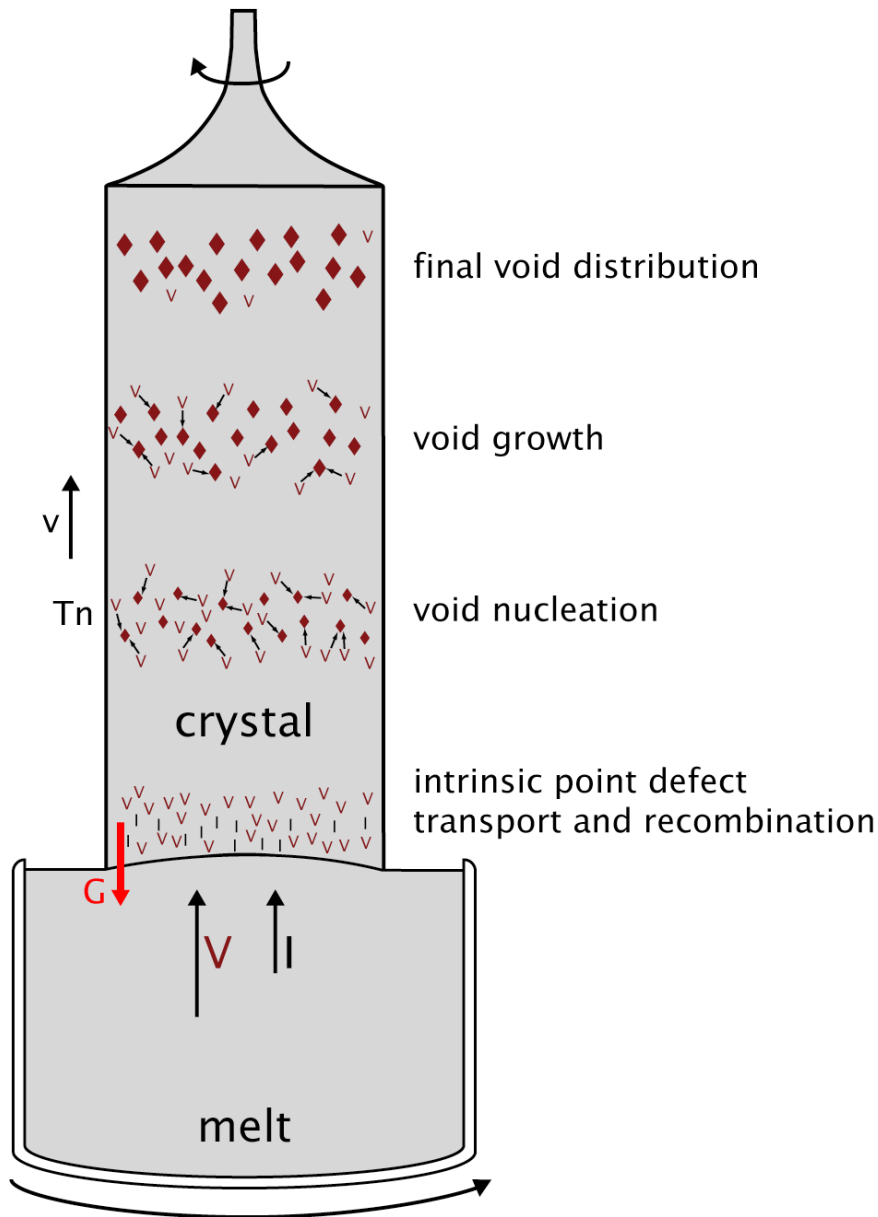


# SEM after coordinate transfer of COP positions



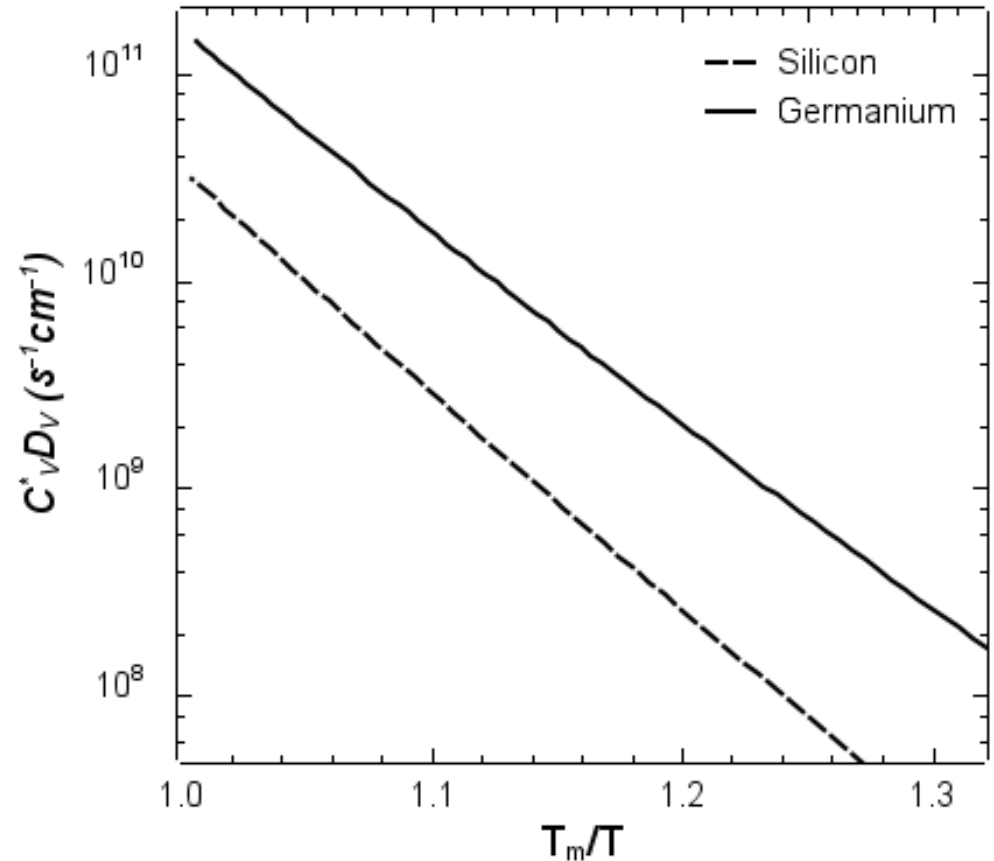
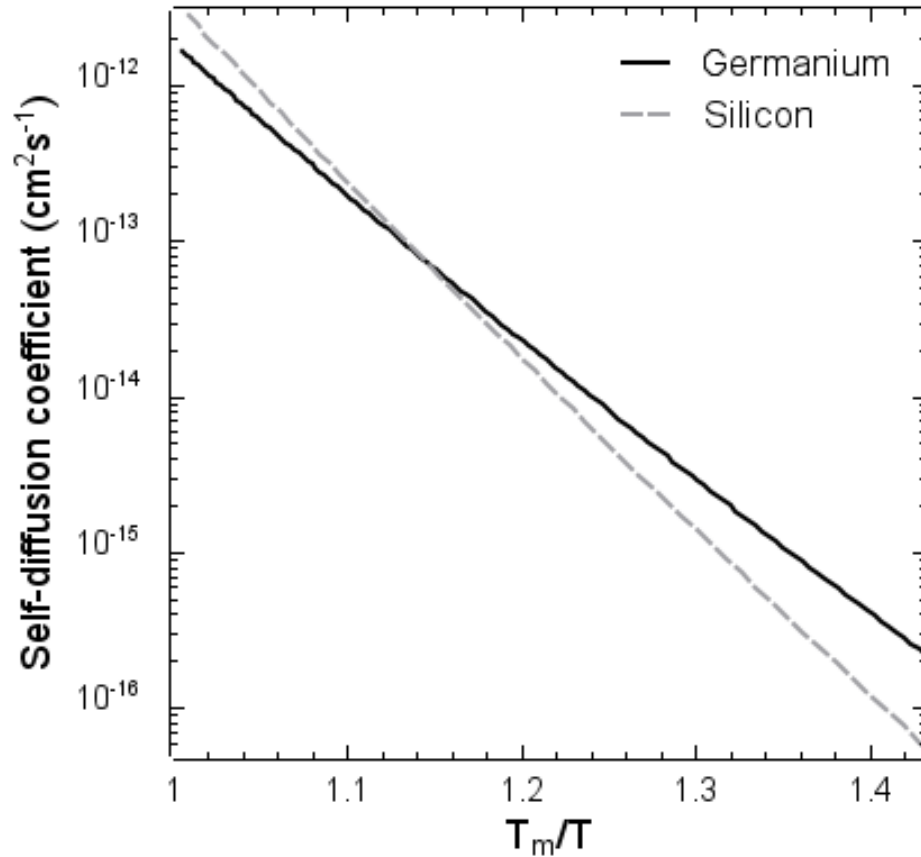
- SEM images of surface pits on Ge wafer surfaces, corresponding with an octahedral (left) and truncated octahedral void (right).

# Void formation in Czochralski germanium

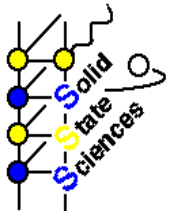


- Schematic view of a growing Ge crystal as a solid-state reactor for point defects.
- Tweet JAP 30, 2002 (1959):
  - pit size depending on thermal history;
  - pit density reduction when pulling slower or post-heating the crystal in the puller;
  - density reduction accompanied by size increase;
  - vacancy clustering mechanism.

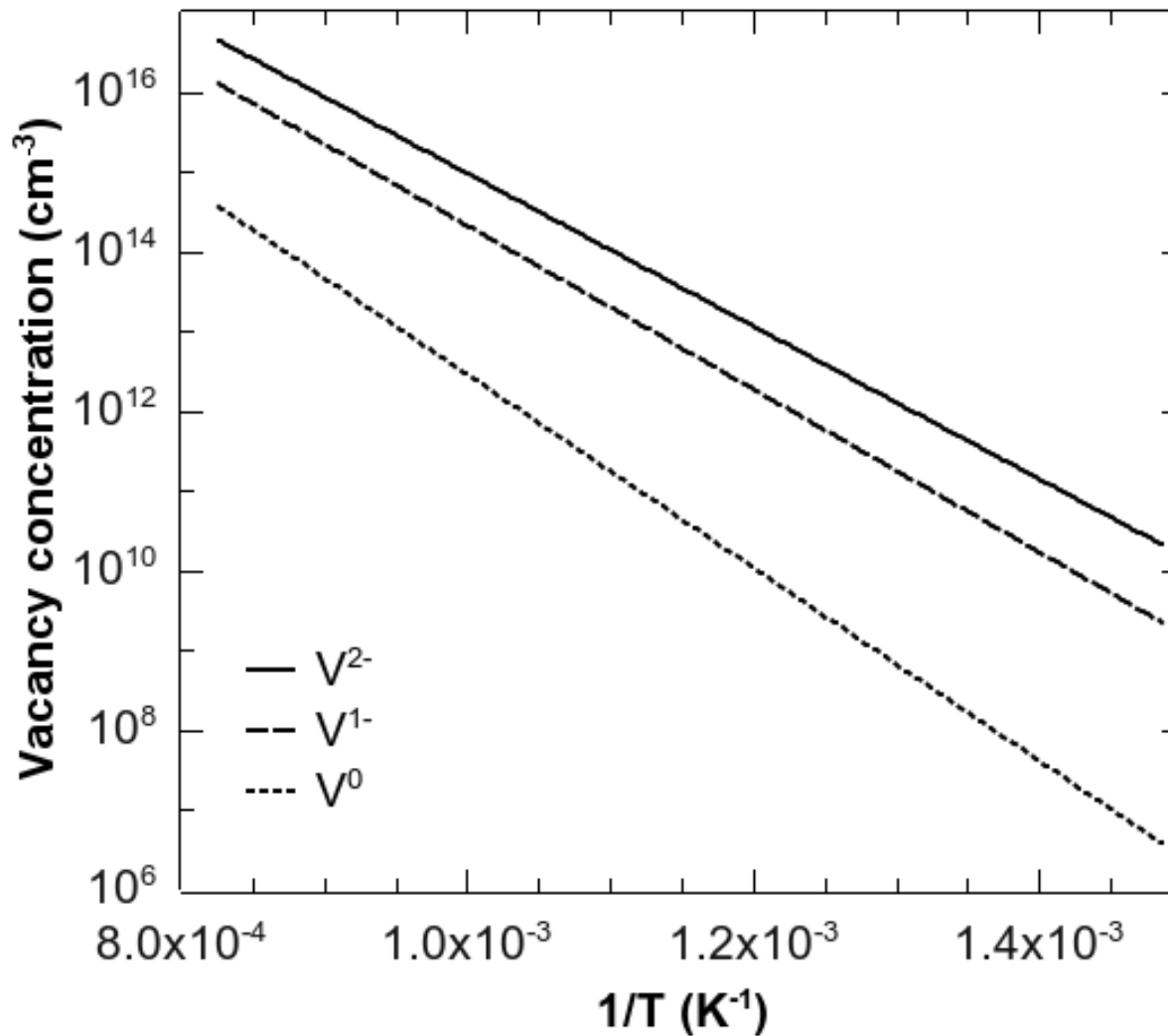
# Self-diffusion and vacancy transport capacity



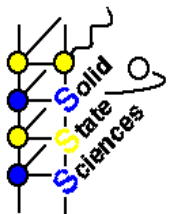
- Self-diffusion coefficient (left) and vacancy transport capacity (right) in Si and Ge as a function of temperature normalized with respect to the melt temperature.



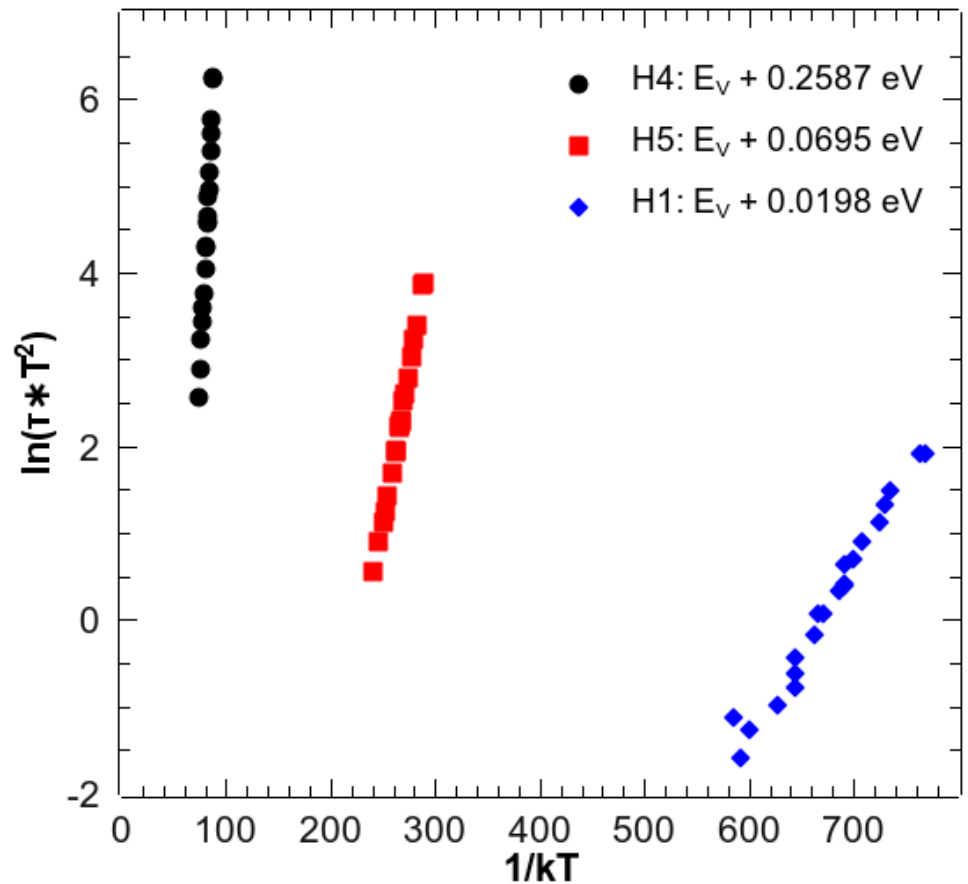
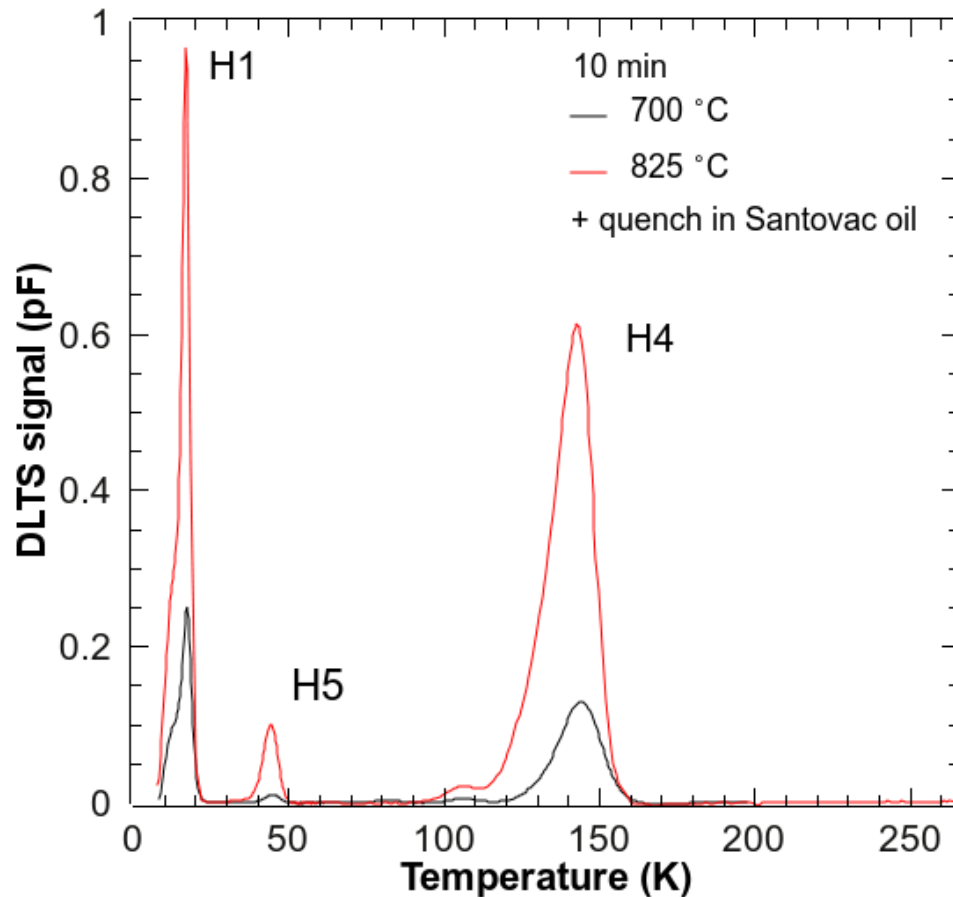
# Vacancies in germanium: quenching experiments



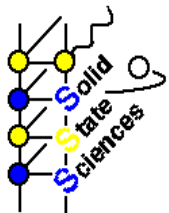
- Thermal equilibrium concentration of different charge states of the vacancy.



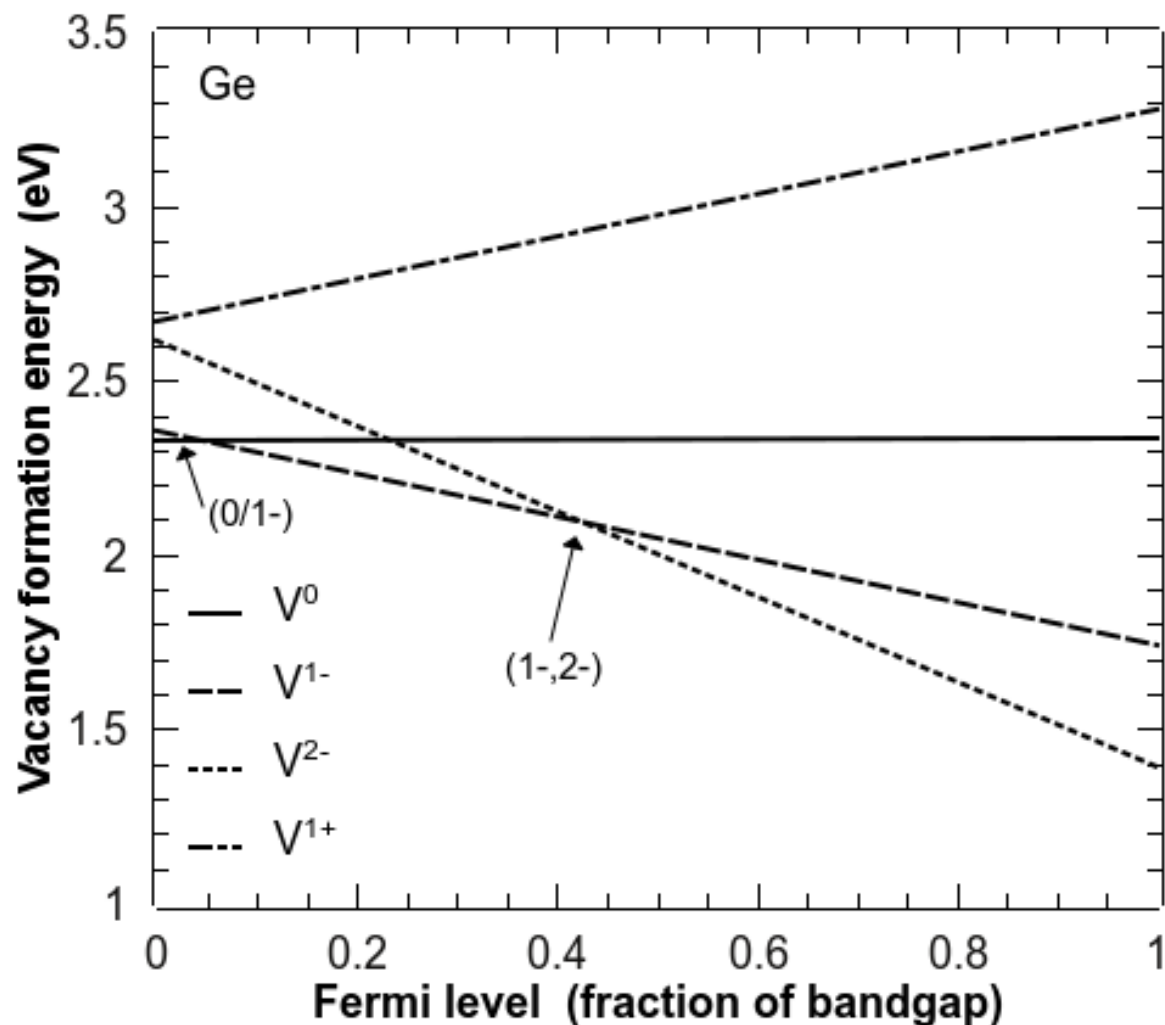
# Quenching experiments: DLTS



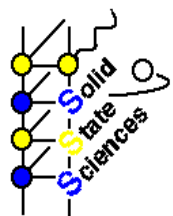
- DLTS spectra measured in quenched samples. No known Cu-related deep levels are observed.



# Ge vacancy formation energy: impact of Fermi level



- Formation energy of the vacancy calculated ab initio with LDA+U as a function of the position of the Fermi level in the bandgap and of the charge state.



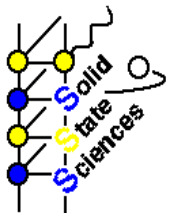
# Charged vacancies in Ge

- Calculated vacancy formation energies in eV ( $E_F = 0.305$  eV).

Charge state	2-	1-	0	1+	2+
LDA+U PAW 3d	2.00	2.05	2.33	2.97	4.01
Quenching	2.19 +/- 0.11	1.98 +/- 0.11	2.35 +/- 0.11	-	-

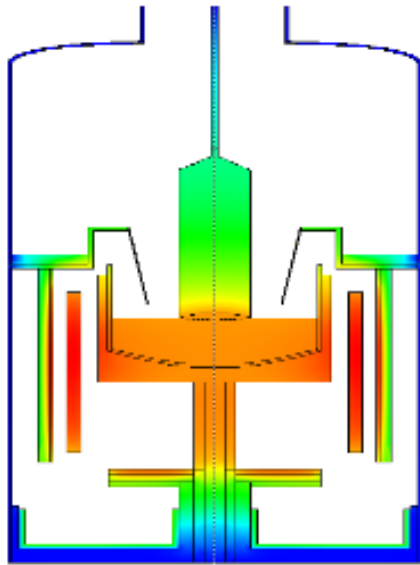
- Acceptor levels in eV for the Ge vacancy.

Reference	0/1-	1-/2-	Method
<b>This work</b>	<b>0.02</b>	<b>0.26</b>	<b>DFT LDA</b>
<b>This work</b>	<b>0.02</b>	<b>0.26</b>	<b>DLTS</b>
Konorova (1969)	0.025 +/- 0.005	0.15 +/- 0.05	Hall effect
Hiraki (1965)	0.03-0.05	0.15 - 0.20	Hall effect
Zhidkov (1961)	0.04	0.25	Hall effect



# Multiscale model for defect dynamics during Cz growth

temperature distribution



**macro scale**

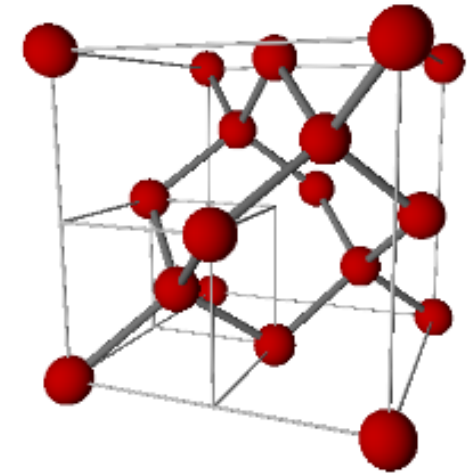
(macroscopic  
process simulation)



**meso scale**

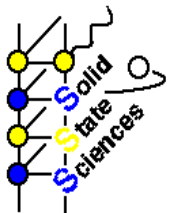
(microscopic defect  
dynamics)

material parameters



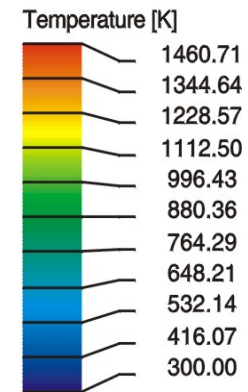
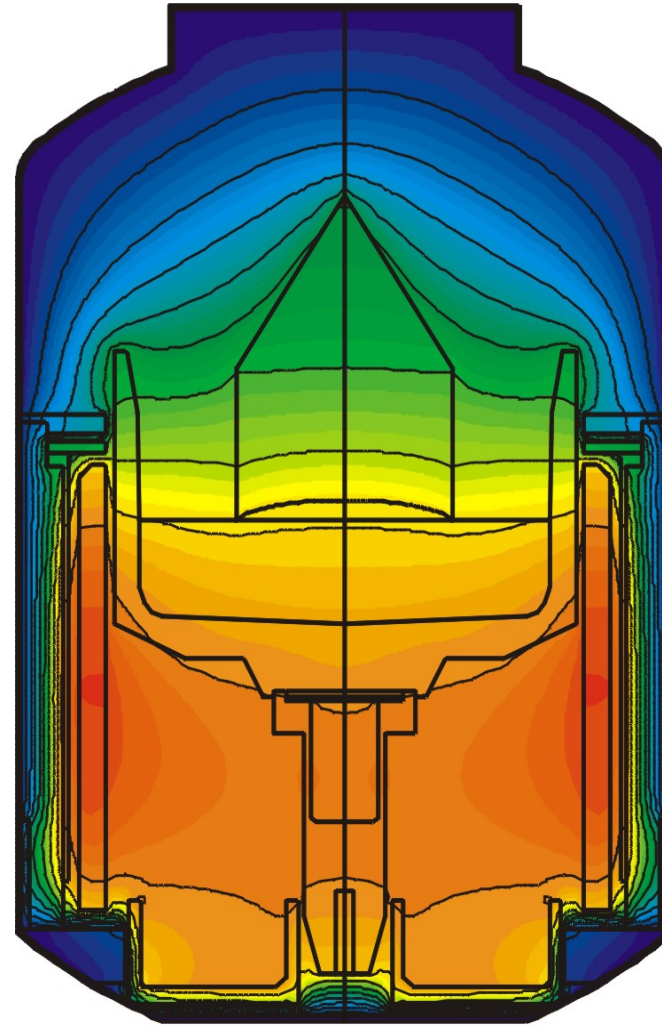
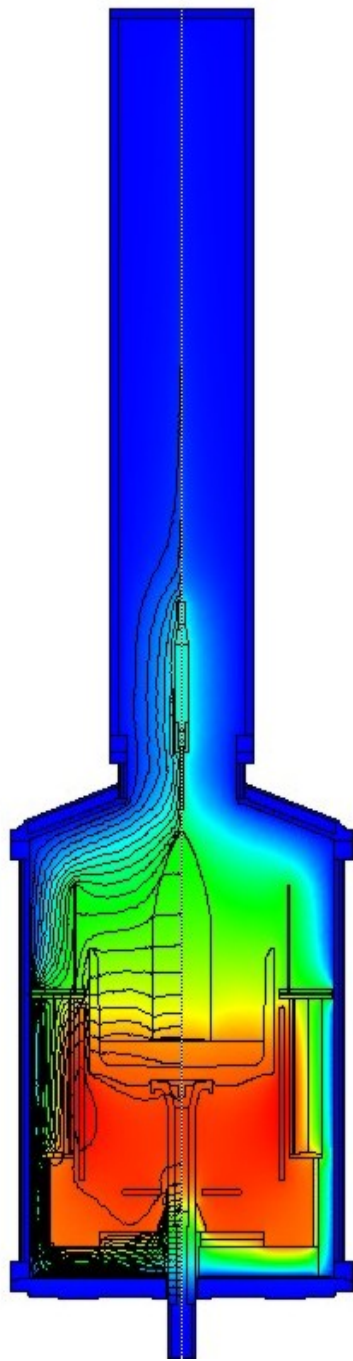
**atomistic scale**

(atomistic models)



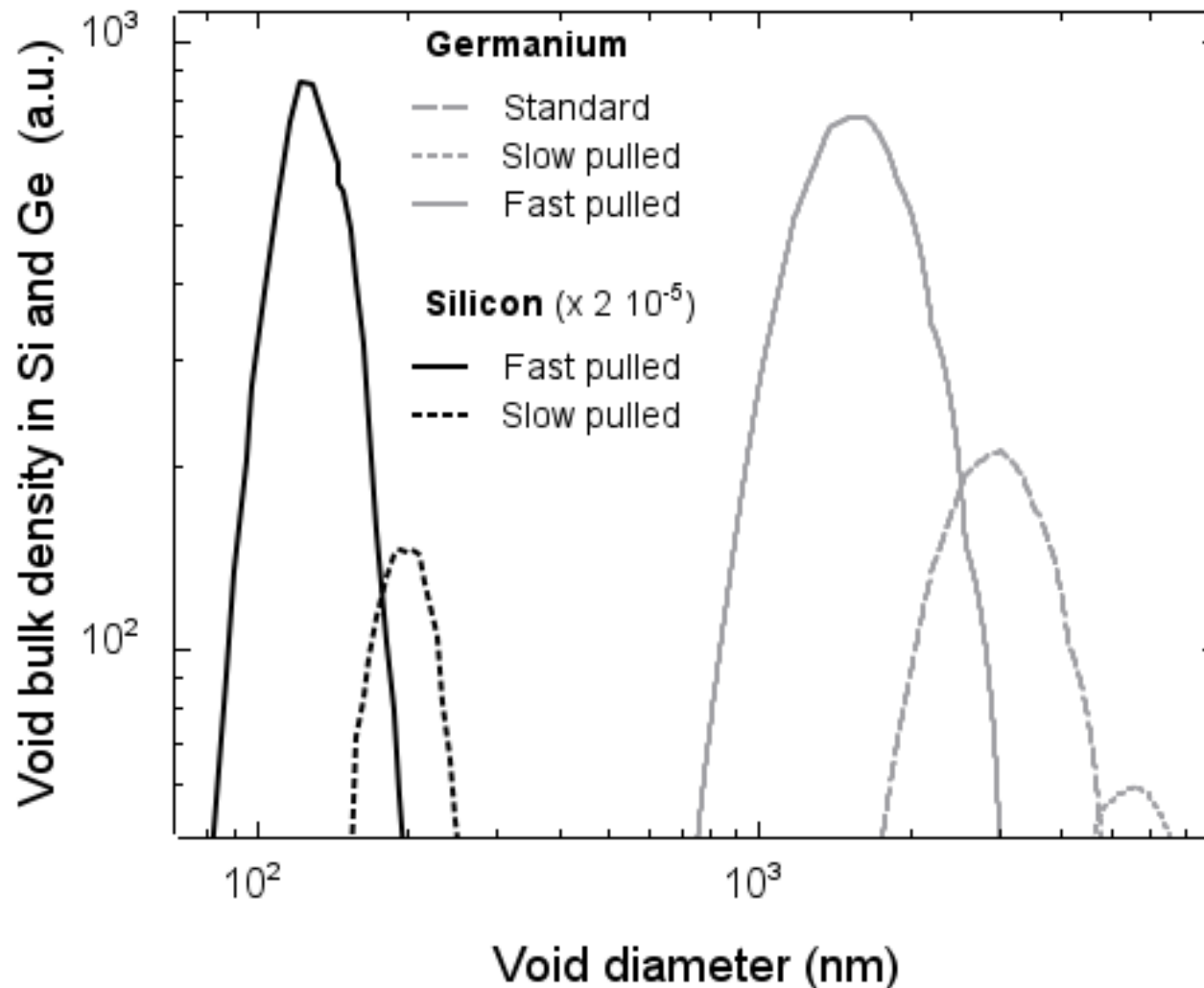


# Thermal simulations



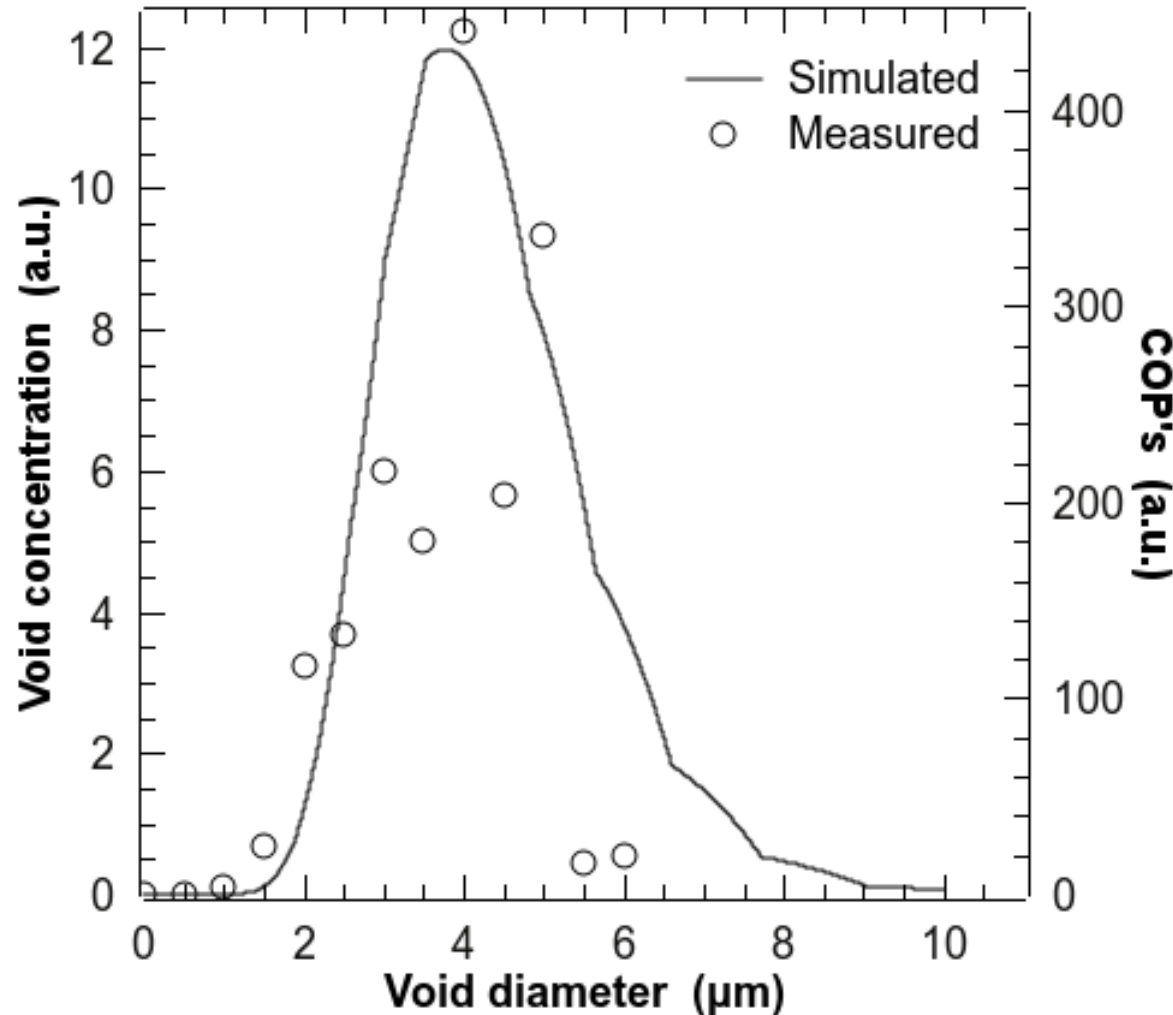
- Thermal simulations of 200 and 300 mm Ge crystal growth.

# Simulation of intrinsic point defect clustering

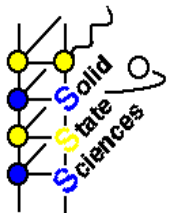


- Simulations illustrating the one order of magnitude larger void size in Ge and the four orders of magnitude lower volume density compared to Si.

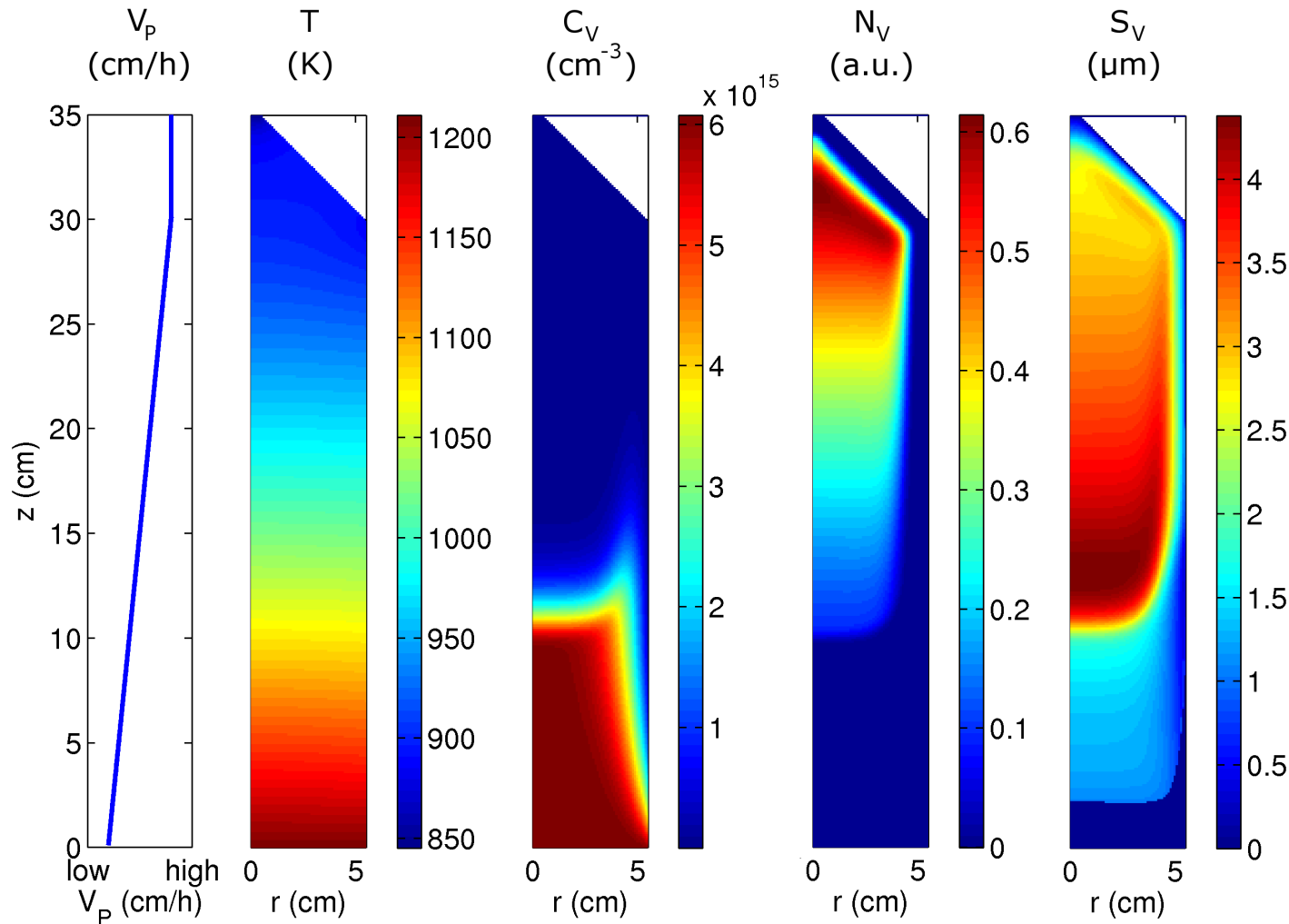
# Simulation of vacancy clustering in Cz Ge



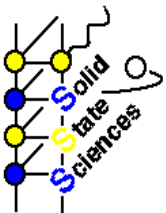
- Comparison between measured COP and simulated void distribution. The COP distribution was measured using a confocal review station.



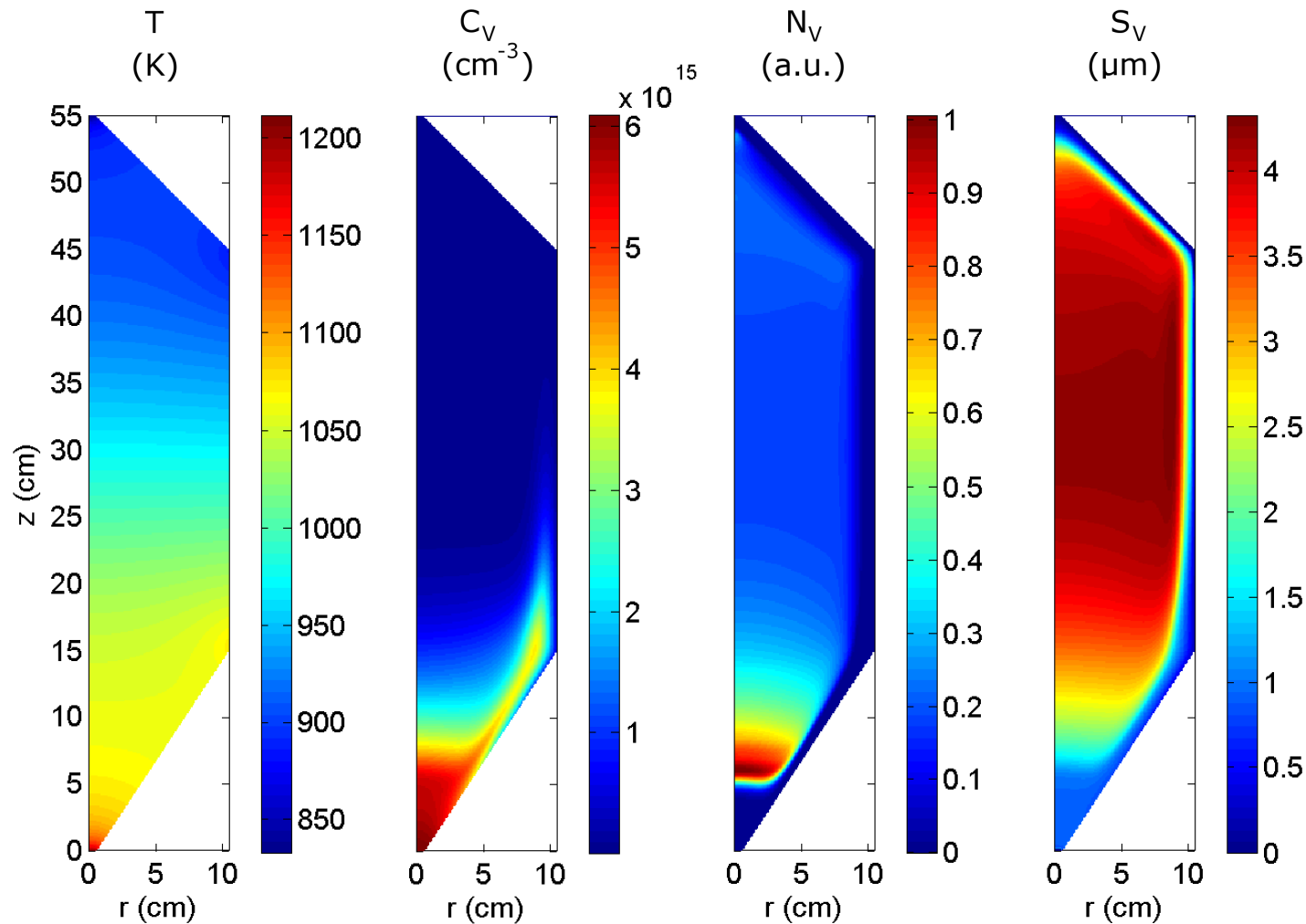
# 2D unsteady-state simulations: decreasing pull rate



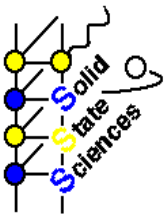
- Temperature, vacancy concentration, vacancy cluster concentration and size distributions for increasing pull rate.



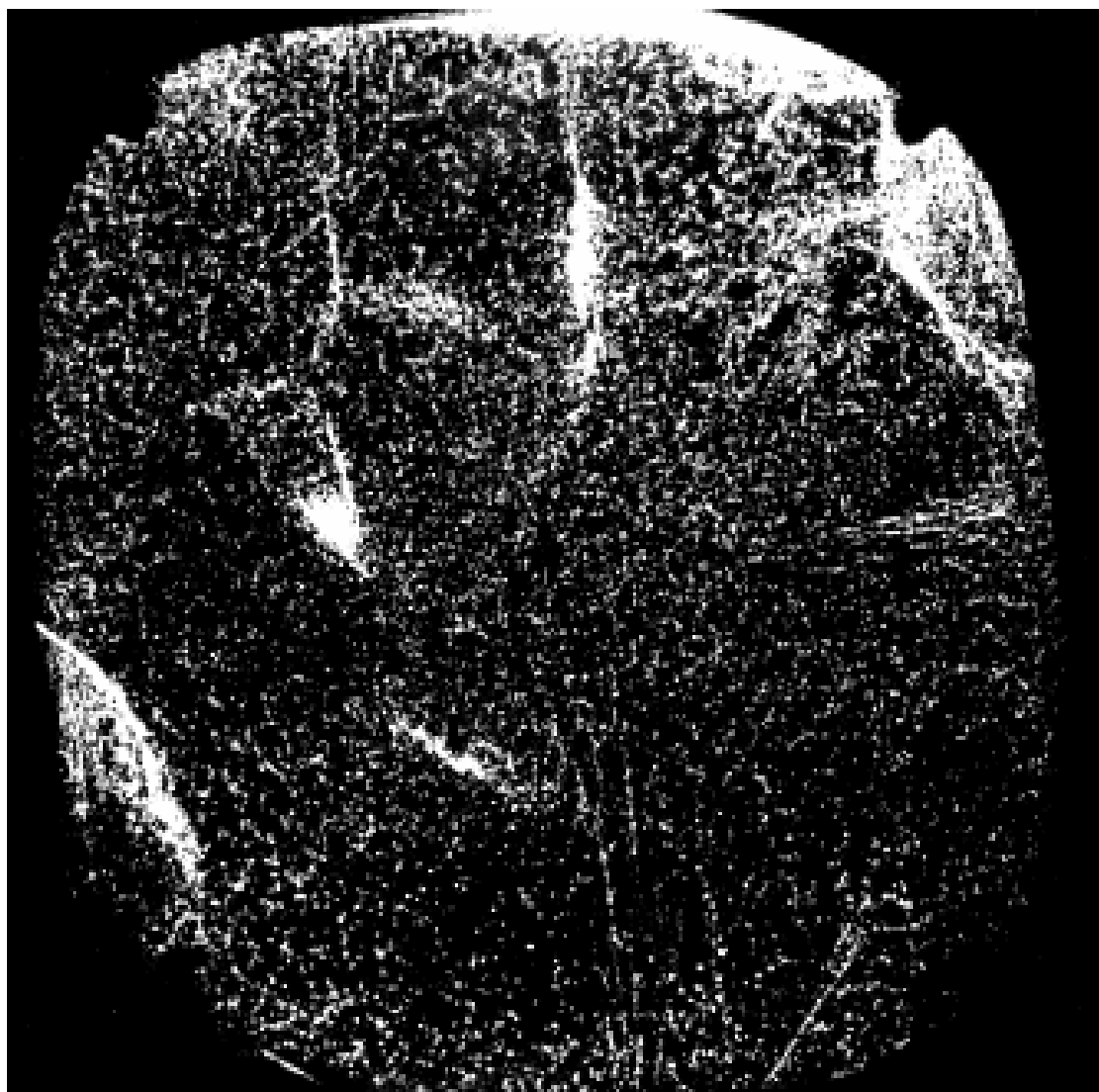
# 2D unsteady-state simulations: full crystal



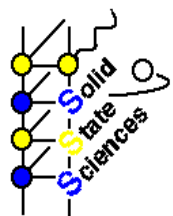
- 2D distributions of  $T$ ,  $V$  concentration,  $V$  cluster concentration and size distribution in a 8'' Ge crystal grown with constant pull rate.



# Epilogue: grown-in dislocations in HR-Ge

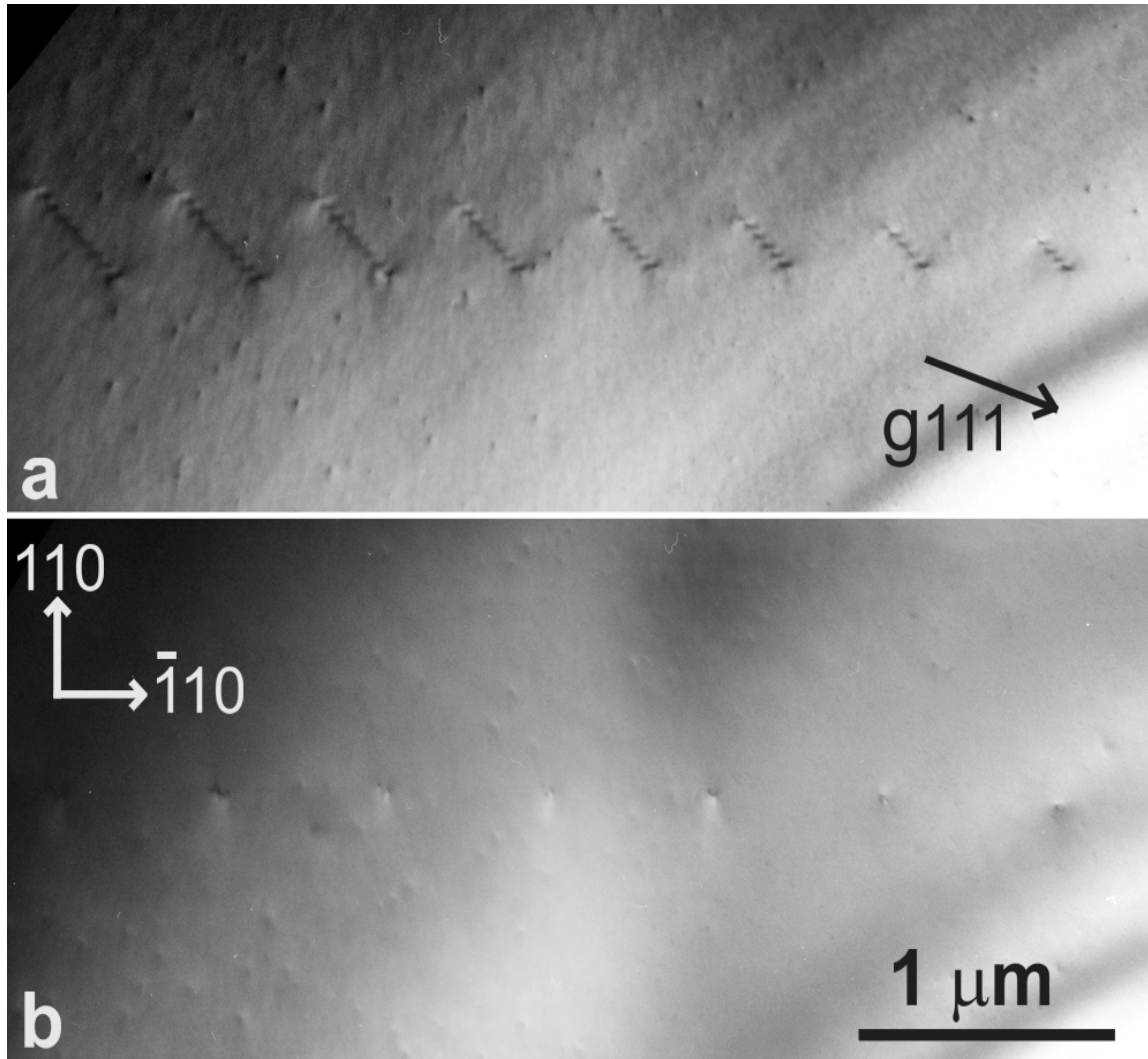


- Optical micrograph of preferentially etched HR-Ge crystal slice revealing dislocation lineage and mosaic structures as well as isolated dislocations.



Van Sande et al, Appl.Phys. A **40**, 257 (1986).

# Grown-in dislocations



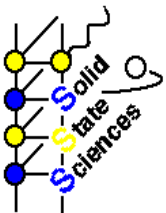
- HVEM of lineage dislocations (Class 1) in a HR germanium crystal. Top) Tilted about  $35^\circ$  away from the  $[001]$  crystal pulling axis. Bottom) The same area viewed along the  $[001]$  axis. Dislocations are seen end-on.

# Epilogue: grown-in dislocations in HR-Ge

- HR-Ge is grown with well defined dislocation density to suppress  $V_2H$  and void formation:
  - 90° (class 1) dislocations form low angle grain boundaries showing up as lineage or mosaic structures of etch pits;
  - 60° (class 2) dislocations: few thousand per  $\text{cm}^2$ ;
  - 30° (class 3) and 90° (class 4) difficult to avoid and radial distribution.
- Dislocation and impurity specs HR Ge crystals:

**Deep Levels** p-type Total Cu concentration, as measured by DLTS :  $\text{Cu}_{\text{tot}} \leq 4,5 \cdot 10^9 \text{ cm}^{-3}$   
 n-type Deep level point defects as measured by DLTS :  $< 5 \cdot 10^8 \text{ cm}^{-3}$

Crystallo- graphic perfection		
	p-type	n-type
Dislocation density (EPD, $\text{cm}^{-2}$ )	$\leq 10000$	$\leq 5000$
Lineage (unit length = slice radius)	$\leq 3$	$\leq 2$
Mosaic structures (unit surface = $100\text{mm}^2$ )	$\leq 5$	$\leq 2$
Saucers ( $\text{cm}^2$ )	$\leq 500$	$\leq 500$





# Conclusions

- The (negatively charged) vacancy is the dominant intrinsic point defect in germanium.
- Quantitative simulation of vacancy introduction and clustering during Czochralski pulling is possible.
- Further work:
  - impact of extrinsic point defects on vacancy thermal equilibrium concentration;
  - experimental data on vacancy and self-interstitial formation energy, diffusivity and recombination;
  - (impact of dislocations).

